Electronic structure of $CeRhIn_5$: de Haas–van Alphen and energy band calculations

Donavan Hall,[1] E. C. Palm,[1] T. P. Murphy,[1] S. W. Tozer,[1] C. Petrovic[1,*] Eliza Miller-Ricci,[1,†] Lydia Peabody,[1,‡] Charis Quay Huei Li,[1,§] U. Alver,[2] R. G. Goodrich,[2] J. L. Sarrao,[3] P. G. Pagliuso,[3] J. M. Wills,[4] and Z. Fisk[1]
[1]*National High Magnetic Field Laboratory, Florida State University, Tallahassee, Florida 32310*
[2]*Department of Physics and Astronomy, Louisiana State University, Baton Rouge, Louisiana 70803*
[3]*Los Alamos National Laboratory, MST-10, Los Alamos, New Mexico 87545*
[4]*Los Alamos National Laboratory, T-1, Los Alamos, New Mexico 87545*
(Received 22 November 2000; published 19 July 2001)

The de Haas–van Alphen effect and energy-band calculations are used to study angular-dependent extremal areas and effective masses of the Fermi surface of the highly correlated antiferromagnetic material $CeRhIn_5$. The agreement between experiment and theory is reasonable for the areas measured with the field applied along the (100) axis of the tetragonal structure, but there is disagreement in size for the areas observed with the field applied along the (001) axis where the antiferromagnetic spin alignment is occurring. Detailed comparisons between experiment and theory are given.

DOI: 10.1103/PhysRevB.64.064506 PACS number(s): 71.18.+y, 71.27.+a

I. INTRODUCTION

The compounds $CeMIn_5$ (M=Co, Ir, Rh) are a newly reported family of heavy fermion superconductors.[1–4] These materials crystallize in the tetragonal $HoCoGa_5$ structure and are built of alternating stacks of $CeIn_3$ and MIn_2. $CeCoIn_5$ and $CeIrIn_5$ have superconducting transition temperatures of 2.3 and 0.4 K, respectively, whereas $CeRhIn_5$ orders antiferromagnetically at 3.8 K at ambient pressure. Applied pressures of order 16 kbar can induce an apparently first-order transition from the magnetically ordered state to a superconducting one with T_c=2.1 K. The particular attraction of these materials is that not only do they represent a substantial increase in the number of known heavy fermion superconductors but also they appear to be quasi-two-dimensional (2D) variants of $CeIn_3$, an ambient-pressure antiferromagnet in which superconductivity can be induced at 25 kbar and 100 mK.[5] If one can demonstrate that the reduced dimensionality is responsible for the factor-of-10 increase in superconducting T_c as well as the anomalous evolution from antiferromagnet to superconductor with pressure, their impact will far exceed that of just another family of heavy-fermion superconductors. However, much work remains to establish this hypothesis.

Because it displays both ''high-temperature'' superconductivity as well as unconventional magnetic behavior, $CeRhIn_5$ seems an ideal candidate for electronic and magnetic spectroscopic probes to establish the degree of reduced dimensionality and its impact on fluctuation spectra. Some progress has been made in establishing the magnetic structure of $CeRhIn_5$.[6,7] Nuclear-quadrupole resonance (NQR) and neutron-diffraction measurements have shown that the magnetically ordered state of $CeRhIn_5$ is a spiral-spin structure in which the spins in a given $CeIn_3$ plane are ordered antiferromagnetically, and the direction of the ordered moments in the plane spirals along the c axis, rotating 107° per layer. Although complete inelastic neutron-scattering measurements of the dynamical susceptibility remain in progress, already NQR has established that the temperature evolution of the sublattice magnetization below T_N is much more rapid than would be expected from mean-field theory and is a sign of reduced dimensionality.

To date, studies of the electronic structure of $CeRhIn_5$ have been far less complete. Cornelius *et al.*[8] have reported limited de Haas–van Alphen (dHvA) measurements along the principal crystallographic axes using pulsed fields. These measurements reveal an anomalous temperature dependence of the dHvA amplitude as well as large directional anisotropies in the effective masses of carriers that have been observed.

Here, we report a more comprehensive dHvA study throughout the entire Brillouin zone of $CeRhIn_5$ and compare our results directly with local-density-approximation band-structure calculations. Recently, a similar study of $CeIrIn_5$ has been reported.[9] Taken together, our results and those of Ref. 9 allow direct evaluation of the changes in electronic properties of $CeMIn_5$ as a function of transition-metal ion M.

In what follows, we report the details of our dHvA measurements and band-structure calculations, discuss the extent to which they are self-consistent, and compare and contrast the electronic structures of $CeRhIn_5$ and $CeIrIn_5$.

II. MEASUREMENTS

All of the measurements reported here were made at the National High Magnetic Field Laboratory, Tallahassee, FL using cantilever magnetometry at temperatures between 20 and 500 mK in applied fields ranging from 5 to 18 T. Complete field rotations in the [100] and [001] planes of the tetragonal structure are reported. The sample was grown from an In flux and etched in a 25% HCl in H_2O solution down to a small plate that was mounted on the cantilever with Apiezon N vacuum grease or GE Varnish. This technique is most sensitive to low-frequency oscillations not observed typically with the magnetic-field modulation technique.

The dHvA effect, a measurement of the oscillatory part of the magnetization, is a method for determining Fermi-surface properties. The oscillatory magnetization M_o is given

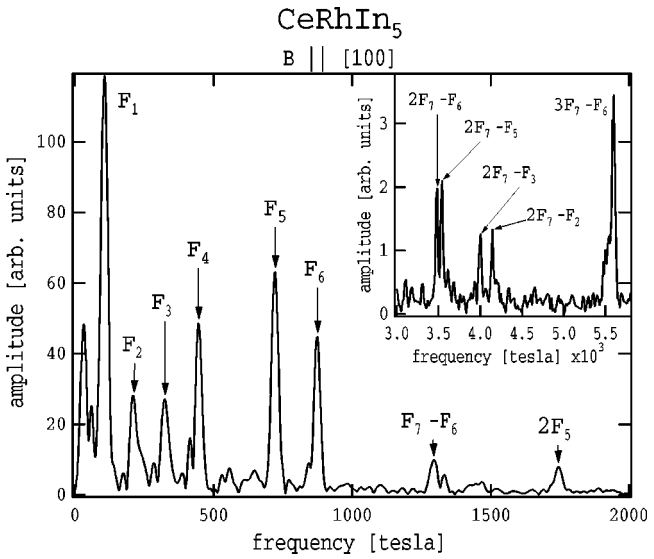

FIG. 1. DFT of dHvA data taken with the applied field parallel to [100]. The inset shows some of the high frequencies that are combinations of the fundamentals.

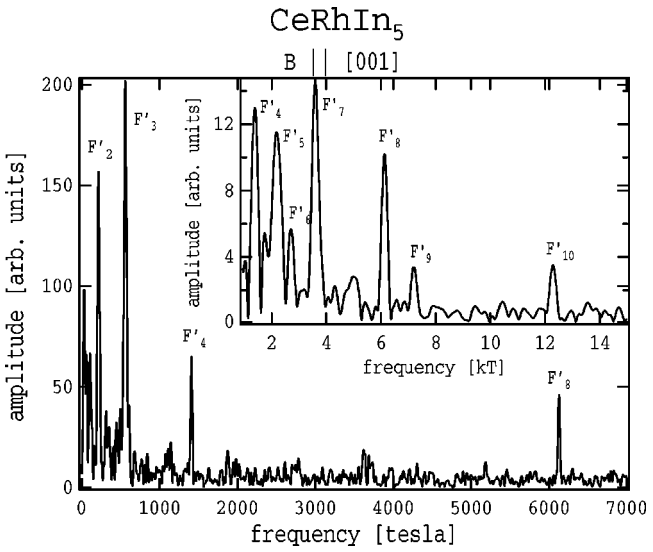

FIG. 2. FFT of dHvA data taken with the applied field parallel to [001].

by the Lifshitz-Kosevitch (LK) equation (see Ref. 10 for the mathematical details),

$$M_o = -2.602\times10^{-6}\left(\frac{2\pi}{HA''}\right)^{1/2}\frac{GFT\exp(-\alpha px/H)}{p^{3/2}\sinh(-\alpha pT/H)}$$

$$\times\sin\left[\left(\frac{2\pi pF}{H}\right)-\frac{1}{2}\pm\frac{\pi}{4}\right], \qquad (1)$$

where $\alpha = 1.47(m/m_0)\times10^5$ G/K, A'' is the second derivative of the area of the Fermi surface (FS) cross section that is perpendicular to the applied field, G is the spin reduction factor, p is the harmonic number, and x is the Dingle temperature. The frequencies of the dHvA oscillations are proportional to extremal areas of the FS and the Fermi-liquid theory works well for heavy-fermion materials as has been shown in previous studies.[11]

Since the magnetization of the sample was measured with a torque cantilever, it is necessary to understand how torque is related to the LK equation. dHvA oscillations in the torque arise from anisotropy in the Fermi surface, such that

$$\tau = \frac{-1}{F}\frac{dF}{d\theta}M_oHV \qquad (2)$$

where F is the dHvA frequency, θ is the angle of the applied field, M_o is given by the LK expression above, and V is the volume of the sample. This means that a roughly spherical FS will have a smaller torque signal than a highly elliptical FS.

Two versions of a Fourier-transform algorithm were used in the analysis: preliminary analysis was done with a fast Fourier transform (FFT) and in some cases a discrete Fourier transform (DFT) was used to increase the frequency resolution. Fourier spectra of the oscillations obtained for the field parallel to [100] and [001] are shown in Figs. 1 and 2. As can be seen, there are several fundamental frequencies and several combinations (especially with the F_7; e.g., $F_7-F_6 = 1302$ T). Similar combination frequencies were found in all field directions; their origins will be discussed below.

The fundamental frequencies are plotted as a function of angle in Fig. 3. As can be seen, the measured frequencies span the range from about 100 T over wide angular ranges to

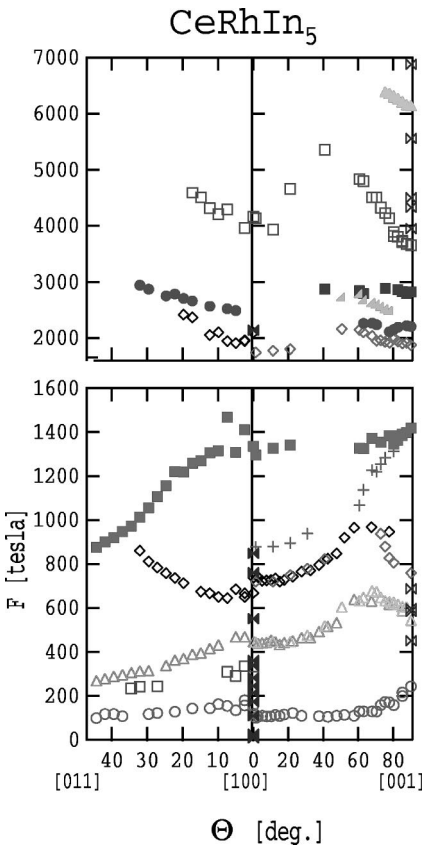

FIG. 3. Frequency as a function of angle. Calculated frequencies for [001] and [100] are indicated with bowties.

TABLE I. Structural parameters of primitive tetragonal $CeRhIn_5$. Calculated parameters were obtained using GGA and Brillouin-zone convergence as discussed in the text. The parameter x is the Wykoff coordinate of displacement of face-centered In atoms along z. Experimental values are from Hegger *et al.*

Space group P4/*mmm*(123)		
V/V_{exp}	1.023	(V_{exp}=163.4 Å^3)
c/a	1.626	(c/a_{exp}1.620)
x	0.302	x_{exp}.306
$B(V_{exp})$	87 GPa	
$B(V_{cal})$	78 GPa	
DOS (E_F)	10.8 eV^{-1}	

5 kT for the field applied near [001]. The one defect of the cantilever technique was alluded to in the previous paragraph—small $dF/d\theta$ produces a small signal amplitude. The measured dHvA oscillations were small for [001] and [100] orientations, and the signal amplitude was maximized at approximately a 45° rotation from each of these principal axes. One might propose that field-modulation measurements would be more appropriate in this case, but given the low (less than 1 kT) frequencies measured here, the required modulation fields are technically impractical in the high-field ranges used.

III. DISCUSSION

The total energy and band structure of $CeRhIn_5$ were calculated with a full-potential electronic structure method that uses linear muffin-tin orbitals as bases.[12] Calculations were performed to obtain theoretical structural parameters, one-electron bands and spectral densities, and the structure of the Fermi surface. All calculations used the generalized gradient approximation (GGA)[13] to treat exchange and correlation and included the spin-orbit interaction in the variational basis. In the range of parameters searched, no magnetic instabilities were found. The calculations reported here are for paramagnetic $CeRhIn_5$ in the simple tetragonal structure (P4/*mmm*).

Structural parameters were obtained by simultaneous variation of volume, c/a, and the single internal structural parameter to minimize the total energy. Substantially converged results were obtained with a set of 45 irreducible (486 total) Brillouin-zone points. The calculated volume, c/a ratio, and internal parameter are given in Table I. Conventional electronic-structure theory (with itinerant Ce $4f$ electrons) applied to a simple paramagnetic cell seems to give a satisfactory description of the structural properties of $CeRhIn_5$. Also given in Table I are the bulk modulus calculated at both the experimental and theoretical volumes and the Density of States (DOS) at the Fermi energy E_F calculated at the experimental volume.

The band structure, calculated at the experimental volume, along high-symmetry lines in the Brillouin zone is shown in Fig. 4. Bands of predominantly Ce $4f$ character dominate the band structure at and just above E_F. The set of bands along $X \rightarrow \Gamma \rightarrow Z \rightarrow R$ are indicative of the nesting

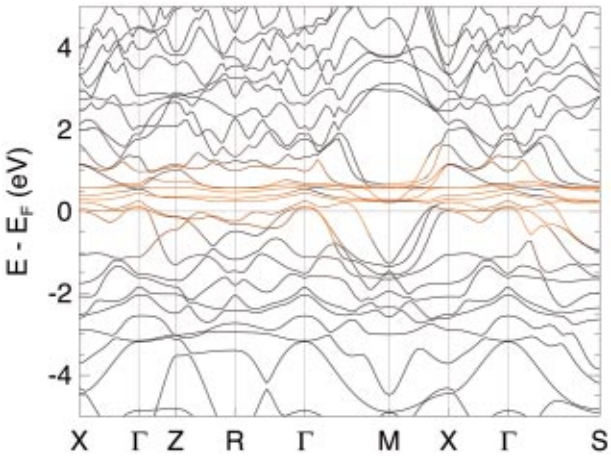

FIG. 4. (Color) The GGA band structure of paramagnetic $CeRhIn_5$ calculated using experimental structural parameters.

found in the Fermi surface discussed below. The electron DOS, shown in Fig. 5, shows the predominance of Ce $4f$ character at the Fermi energy. The DOS at E_F, while fairly large, does not indicate a dramatic structural instability.

Fermi surfaces were calculated using a fine mesh (4800 irreducible points, corresponding to a $48\times48\times32$ gridding of the Brillouin zone) with a potential converged with 270

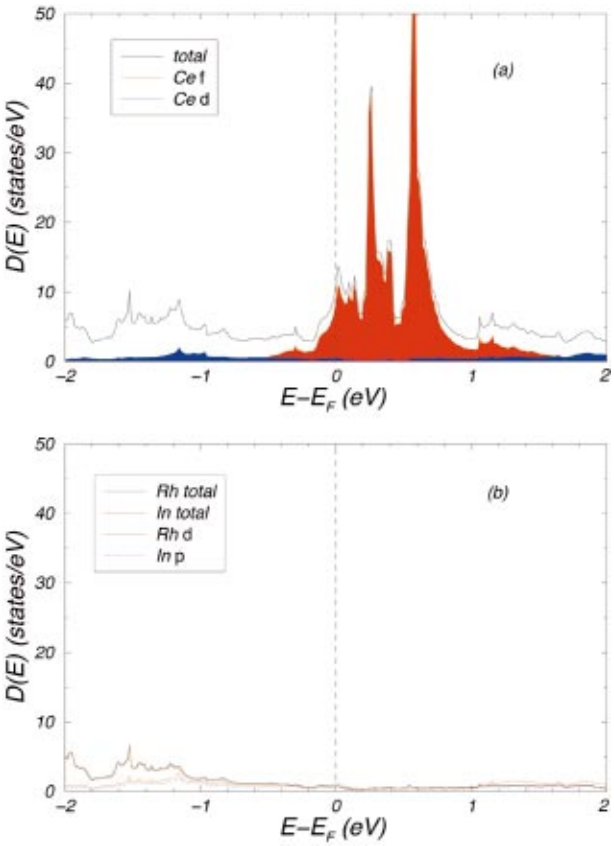

FIG. 5. (Color) The GGA density of states of paramagnetic $CeRhIn_5$ calculated using experimental structural parameters. Ce $4f$ and $5d$ projections are shown in (a) and Rh and In projections are shown in (b).

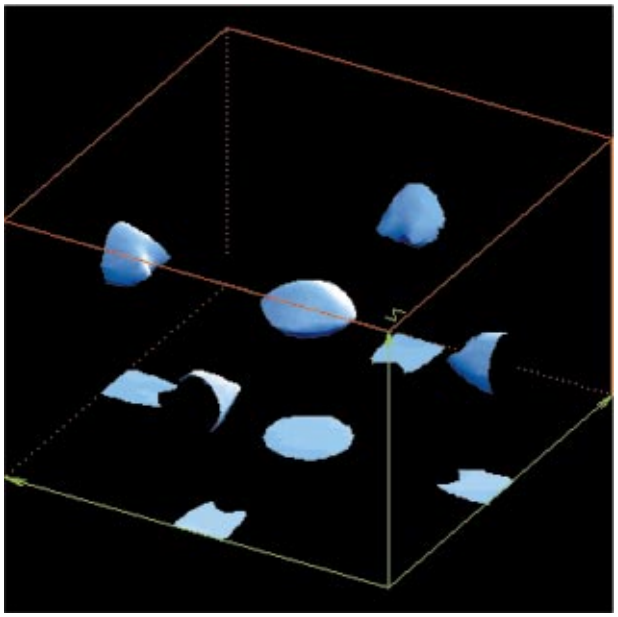

FIG. 6. (Color) The first sheet of the paramagnetic $CeRhIn_5$ Fermi surface. The electron surface is illuminated; these are hole surfaces.

irreducible Brillouin-zone points. Three doubly degenerate bands, which we label band 90, band 92, and band 94, cross the Fermi energy. The Fermi surface sheets formed by these three bands are shown in Figs. 6, 7, and 8. In the figures, Γ, the center of the conventional Brillouin zone, is at the origin, i.e., at the corners of the cubes. The lowest energy sheet, band 90, shown in Fig. 6, consists of hole surfaces centered around Γ and X giving relatively low ($\lesssim 600$ T) dHvA frequencies. The next sheet, shown in Fig. 7, has both hole and electron surfaces stretched along the tetragonal axis. The last

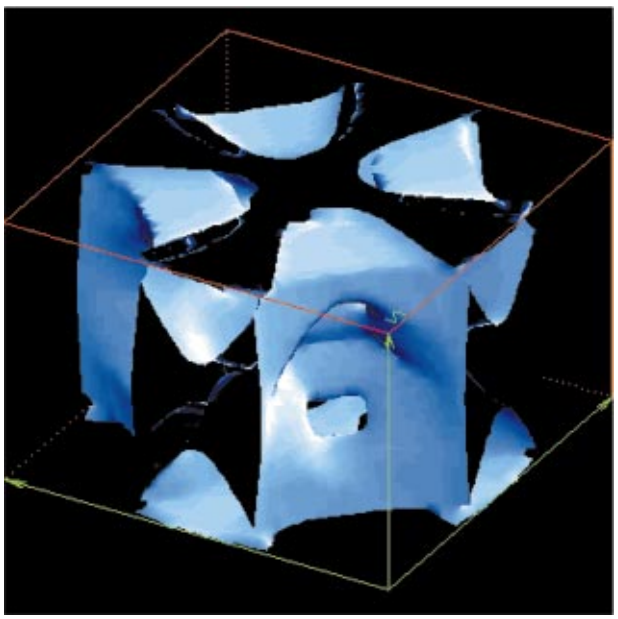

FIG. 7. (Color) The second sheet of the paramagnetic $CeRhIn_5$ Fermi surface. The electron surface is illuminated.

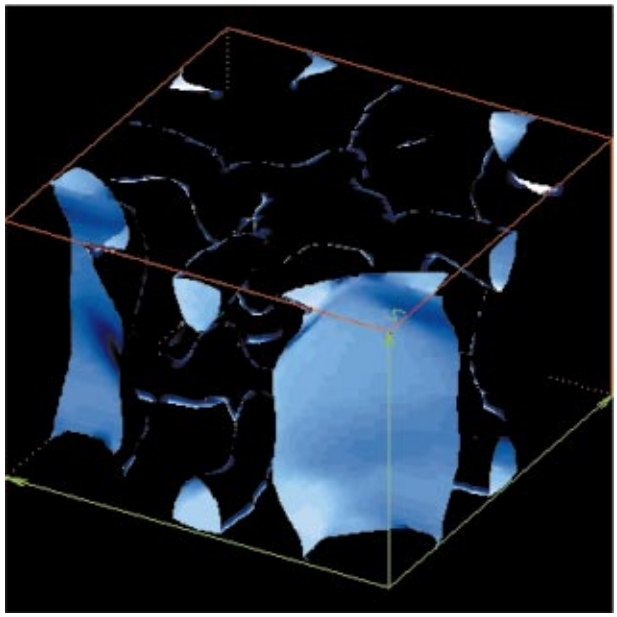

FIG. 8. (Color) The third sheet of the paramagnetic $CeRhIn_5$ Fermi surface. The electron surface is illuminated.

sheet, shown in Fig. 8, is predominantly an electron surface, although there is a large-area ([001]) hole surface on that sheet. This sheet consists of cylinders surrounding [001] axis and a lattice-structure surface. The dHvA frequencies corresponding to extremal areas are given in Tables II and III.

We measured the temperature dependence of the dHvA amplitudes in the primary crystallographic directions. We did not observe the anomalous temperature dependence of the dHvA amplitudes noted in Ref. 8, where for $B\|$ [001] the amplitudes of the oscillations increase with increasing tem-

TABLE II. Measured and calculated dHvA frequencies for $CeRhIn_5$ with $\vec{B}$ along [100]. Frequencies listed by Cornelius have been corrected by 4.5% (Ref. 16).

Calc. F (T)	Band	F (T)	Symb.	F (T)[8]
2139	92 (h)	2176	F_7	
849	92 (e)	874	F_6	861
761	92 (e)	722	F_5	714
551	92 (h)	446	F_4	492
362	90 (h)			
342	90 (h)			
337	90 (h)	324	F_3	295
283	94 (e)			
245	90 (h)			
214	94 (e)	212	F_2	219
175	94 (e)			
110	94 (e)	106	F_1	105
26	92 (h)			
22	90 (h)			
21	92 (h)			
10	90 (h)			
9	90 (h)			

TABLE III. Measured and calculated dHvA frequencies for $CeRhIn_5$ with $\vec{B}$ along [001].

Calc. F (T)	Band	Meas. F (T)	Symb.	F (T), Refs. 8 and 16
12 326	92 (e)	12 280	F'_{10}	
12 126	92 (e)			
11 268	94 (h)			
6878	92 (e)	7200	F'_9	
5562	94 (e)	6120	F'_8	6256
4502	94 (e)	3600	F'_7	3605
4331	94 (e)	2740	F'_6	
3951	94 (e)	2160	F'_5	
686	90 (h)	1412	F'_4	
597	90 (h)	562	F'_3	
585	90 (h)	216	F'_2	
451	90 (h)	(115)	F'_1	

peratures between 0.4 and 1.2 K then decrease. Our measurements carried out between 25 and 500 mK show decreasing amplitudes with increasing temperature in all cases.

The measurements reported here agree substantially with Cornelius *et al.*[8] after a 5% correction to their data;[16] all but one (4708 T) of the frequencies reported in Ref. 8 are observed here also. One major difference is the measurements along [001] where we see many more frequencies. Our measured frequencies in this direction run low as compared to calculations, but we share two frequencies measured by Cornelius *et al.*: our F'_7 and F'_8 (see Table III, Ref. 16). Also, the masses we measure for these orbits are in excellent agreement (see Table V). Cornelius *et al.* report a high-mass orbit at 4686 T, which we do not see. Another major difference is that our measured masses for [100] are higher when compared with those of Cornelius *et al.* (see Table IV), a fact consistent with our nonobservance of the anomalous temperature dependence.

IV. COMPARISON OF EXPERIMENT WITH THEORY

We start the comparison between the calculated frequencies and the measured frequencies with those calculated and observed for the field along the [100] direction. In this case there are many more measured frequencies than the calculated FS gives. We attribute this situation to strong magnetic interactions between electrons on different parts of the FS or

TABLE IV. Measured masses for dHvA frequencies for $CeRhIn_5$ with $\vec{B}$ along [100]. Our data also are compared to that of Cornelius *et al.*

Symb.	F (T)	$m^*(m_e)$	F (T)[8]	$m^*(m_e)$, Ref. 8
F_6	874	3.3 ± 0.6	861	1.31 ± 0.22
F_5	722	2.0 ± 0.8	714	1.17 ± 0.09
F_4	446	3.9 ± 0.9	492	0.72 ± 0.14
F_3	324	5.5 ± 1.0	295	0.93 ± 0.15
F_2	212	2.9 ± 0.4	219	0.99 ± 0.10
F_1	106	3.3 ± 0.6	105	1.36 ± 0.23

TABLE V. Measured dHvA frequencies for $CeRhIn_5$ with $\vec{B}$ along [001]. The frequency in parentheses is weak due to a low number of oscillations in the sweep range.

Symb.	F (T)	$m^*(m_e)$	F (T), Ref. 8	$m^*(m_e)$, Ref. 8
F'_{10}	12 280[a]			
F'_9	7200[a]			
F'_8	6120	6.1 ± 0.3	6256	6.5 ± 0.8
F'_7	3600	4.6 ± 1.0	3605	4.8 ± 0.4
F'_6	2740[a]			
F'_5	2160[a]			
F'_4	1412	4.5 ± 0.3		
F'_3	562[b]			
F'_2	216[b]			
F'_1	(115)[b]			

[a]These frequencies appear only at the lowest temperatures.

[b]Calculation of masses for these frequencies was not possible because the amplitudes did not change significantly over the measured temperature range.

to torque interactions due to the use of the cantilever. Either of these effects can give rise to a series of frequencies that are combinations of two fundamental frequencies.[10] The measured fundamental frequencies in Table II are indicated as F_1–F_7, and some of the combinations that are differences between the fundamentals or harmonics of a fundamental and another fundamental frequency are shown in Fig. 1. It should be noted that the same fundamental frequencies are subtracted from both the fundamental 2176 T and the first two harmonics of 2176 T (F_7) to give the observed combination frequencies (see the inset in Fig. 1). In one case, 1744 T is the first harmonic of the fundamental 874 T (F_6) frequency.

Five frequencies ranging from 9 to 26 T obtained in the band calculations are too low to be observed experimentally. That is, in the field range where oscillations are observed (from about 7 to 18 T) there are too few oscillations for these frequencies to be measurable. In addition there are four electron orbits grouped into two pairs, 245 T and 215 T, 175 T and 110 T, for which we observe only two frequencies, 212 T and 106 T. Again, the Fourier transform may not have sufficient resolution due to an insufficient number of oscillations to resolve all of these frequencies.

The remaining five measured frequencies are in the same range as the predicted frequencies from the band calculation. Differences in detail occur, but it appears that for the field in this direction the measurements give strong support to the predicted FS.

The agreement between the calculated and measured frequencies is not as good for the field in the [001] direction. There are three calculated high frequencies, 11.268 kT, 12.126 kT, and 12.326 kT, whereas only one frequency in this range is observed, 12.280 kT. This high frequency only is observed in the lowest temperature data, 20 mK, and indicates a large effective mass for this frequency. The fact that only one rather than three frequencies are observed may indicate that the electron surface is much more cylindrical

than is obtained from band theory. For the remainder of the frequencies, only the total number and order of the observed frequencies agree with the calculations.

In the band calculation the fact that the sample is antiferromagnetic at low fields in all of the measurement temperature ranges has not been taken into account. In the model that has been taken for the band calculations, the Ce $4f$ electron is completely itinerant and there are no localized moments to cause the magnetism. Therefore, it is most likely that spin-density waves exist in the electronic system and drastically alter the FS. This is the accepted situation in Cr,[14] and may be the case here. A much more involved theory is required to predict the FS under these circumstances. Exchange interactions could cause the FS to be split into separate spin-up and spin-down sheets. In order for this to be determined from dHvA measurements several harmonics of these frequencies would have to be measured.[15] We did not observe the harmonics in these measurements and need to make measurements to higher fields at milliKelvin temperatures to do so.

V. COMPARISON OF $CeRhIn_5$ WITH $CeIrIn_5$

The structure of the Fermi surface of $CeRhIn_5$ is essentially the same as that calculated for $CeIrIn_5$ by Haga *et al.*[9] except that the frequency of the hole orbit perpendicular to [001] arising from (what we label) band 94 near Γ is $\sim 11\,000$ T, rather than $\sim 15\,000$ T reported in Ref. 9. Our own calculations for $CeIrIn_5$ find a frequency close to that calculated for $CeRhIn_5$, $\sim 11\,600$ T.[17] The high frequency reported in Ref. 9 was not seen experimentally. The difference in the two calculations may be in our inclusion of the spin-orbit interaction or in the fineness of the grid used to calculate the Fermi surface.

The dHvA measurements on $CeIrIn_5$ (Ref. 9) find eight branches for rotations in the [100] and [110] planes of the tetragonal structure. Most of these branches are associated with large quasi-2D undulating cylinders that show the expected $1/\cos(\theta)$ dependence of the measured frequencies with θ being the angle at which the field is applied away from the [100] axis. We see a similar behavior in the high frequency orbits for $CeRhIn_5$. Band-structure calculations predict, in Refs. 9 and 17, in addition, that several small pieces of FS should exist in both $CeRhIn_5$ and $CeIrIn_5$. These frequencies were not observed in Ref. 9 for $CeIrIn_5$ but are observed here in $CeRhIn_5$. These differences likely are a result of the measurement techniques employed and not of differences in the actual Fermi surfaces of the respective materials. Overall, the result of these angular-dependent dHvA measurements on $CeRhIn_5$ along with the band calculations show that the Fermi surface has both small pockets of 3D character and large undulating cylinders that should give rise to a 2D character in other properties.

From the temperature dependence of the signal amplitudes we have calculated the effective masses of the observed frequencies in cases where signals were observable over the entire temperature range of measurement. There are two cases where no masses are reported: (1) for F_1'–F_3' in Table V the masses are sufficiently light that we observe no amplitude change within measurement uncertainty up to 0.5 K and (2) for F_7 in Table II and F_5', F_6', F_9', and F_{10}' in Table III, the signals are observed only at the lowest temperatures. The masses are obtained from fits to the Dingle reduction factor in Eq. (1),

$$R_T = \pi\lambda/\sinh(\pi\lambda), \tag{3}$$

where $\lambda = 2\pi pkT/\beta B$, $\beta = eh/(m/m_0)c$, and $m/m_0 = m^*$ is the effective mass. All of the effective masses we obtain in this manner are greater than 1, and compare favorably to the values found in Ref. 8 from the high-temperature dHvA data. We note that none of the measured masses are sufficiently large to account for the measured value of Γ of 400 mJ/mole K from high-temperature specific-heat measurements.[8] On the other hand there is a loss of entropy due to magnetic ordering and the inferred value of Γ below T_N is 56 mJ/mole K, much more in line with the masses reported here. The effective masses measured on $CeIrIn_5$ (Ref. 9) are larger than what we observe in $CeRhIn_5$, consistent with the larger value of Γ measured in $CeIrIn_5$ (Ref. 2) (in which no magnetic order is observed).

VI. CONCLUSION

We have determined the electronic structure of $CeRhIn_5$. This determination includes both the results of dHvA measurements and energy-band calculations. The major findings are as follows.

(1) The Fermi surface consists of structures arising from two hole bands and one electron band. The band calculations assume a completely itinerant $4f$ electron from the Ce atoms and the measurements confirm this assumption. One of the hole surfaces and the electron surface are open along the *c* axis and could give rise to some rather two-dimensional character to the electronic properties.

(2) While the energy-band calculations are for paramagnetic $CeRhIn_5$ and the measurements are on antiferromagnetic $CeRhIn_5$, the agreement between experiment and theory is good for electron areas perpendicular to the *a*-*b* plane, but deviate in size for orbits in this plane. This disagreement is thought to be due to spin-density waves in the *c*-axis direction that give rise to the antiferromagnetism in the *a*-*b* plane.

(3) The electronic effective masses that are measured all are greater than the free-electron mass and are anisotropic, varying from less than m_0 to $6m_0$ depending on direction.

Overall, the Fermi surface of antiferromagnetic $CeRhIn_5$ is similar to that found previously[9] in superconducting $CeIrIn_5$. Thus, while their ambient-pressure ground states are completely different, both of these materials have large electron-electron interactions and rather similar electronic structures.

ACKNOWLEDGMENTS

This work was supported in part by the National Science Foundation under Grant No. DMR-9971348 (Z.F.). A portion of this work was performed at the National High Magnetic Field Laboratory, which was supported by NSF Cooperative Agreement No. DMR-9527035 and by the State of Florida. Work at Los Alamos was performed under the auspices of the U.S. Department of Energy.

*Present address: Ames Laboratory, U. S. Department of Energy and Department of Physics and Astronomy, Iowa State University, Ames, Iowa 50011.
†Present address: EMR, Middlebury College, Middlebury, VT 05753.
‡LP, Smith College, Northampton, MA 01063.
§CQHL, Mount Holyoke College, South Hedley, MA 01075.

[1] H. Hegger, C. Petrovic, E. G. Moshopoulou, M. F. Hundley, J. L. Sarrao, Z. Fisk, and J. D. Thompson, Phys. Rev. Lett. **84**, 4986 (2000).
[2] C. Petrovic, P. G. Pagliuso, M. F. Hundley, R. Movshovich, J. L. Sarrao, J. D. Thompson, and Z. Fisk, Europhys. Lett. **53**, 354 (2001).
[3] C. Petrovic, P. G. Pagliuso, M. F. Hundley, R. Movshovich, J. L. Sarrao, J. D. Thompson, Z. Fisk, and P. Monthoux, J. Phys.: Condens. Matter **13**, L337 (2001).
[4] J. D. Thompson, R. Movshovich, N. J. Curro, P. C. Hammel, M. F. Hundley, M. Jaime, P. G. Pagliuso, J. L. Sarrao, C. Petrovic, Z. Fisk, F. Bouquet, R. A. Fisher, and N. E. Phillips, cond-mat/0012260 (unpublished).
[5] N. D. Mathur, F. M. Grosche, S. R. Julian, I. R. Walker, D. M. Freye, R. K. W. Haselwimmer, and G. G. Lonzarich, Nature (London) **394**, 39 (1998).
[6] N. J. Curro, P. C. Hammel, P. G. Pagliuso, J. L. Sarrao, J. D. Thompson, and Z. Fisk, Phys. Rev. B **62**, R6100 (2000).
[7] W. Bao, P. G. Pagliuso, J. L. Sarrao, J. D. Thompson, Z. Fisk, J. W. Lynn, and R. W. Erwin, Phys. Rev. B **62**, R14 621 (2000).
[8] A. L. Cornelius, A. J. Arko, J. L. Sarrao, Z. Fisk, and M. F. Hundley, Phys. Rev. B **62**, 14 181 (2000).
[9] Y. Haga, Y. Inada, H. Harima, K. Oikawa, M. Murakawa, H. Nakawaki, Y. Tokiwa, D. Aoki, H. Shishido, S. Ikeda, N. Watanabe, and Y. Onuki (unpublished).
[10] D. Shoenberg, *Magnetic Oscillations in Metals* (Cambridge University Press, Cambridge, 1984).
[11] A. Wasserman and M. Springford, Adv. Phys. **45**, 471 (1996).
[12] J. M. Wills, O. Eriksson, and M. Alouani, *Electronic Structure and Physical Properties of Solids*, edited by Hugues Dreyssè (Springer-Verlag, Berlin, 2000), p. 148.
[13] J. P. Perdew, K. Burke, and M. Ernzerhof, Phys. Rev. Lett. **77**, 3865 (1996).
[14] Eric Fawcett, Rev. Mod. Phys. **60**, 209 (1988).
[15] A. Telklu, R. G. Goodrich, N. Harrison, D. Hall, Z. Fisk, and D. Young, Phys. Rev. B **62**, 12 875 (2000).
[16] Due to further data analysis by A. L. Cornelius (private communication).
[17] Similar calculations for $CeIrIn_5$ were done by J. M. Wills in the course of obtaining the $CeRhIn_5$ results reported here.